Available online at www.sciencedirect.com

SciVerse ScienceDirect

Ceramics International 39 (2013) 8543–8548

CERAMICS INTERNATIONAL

www.elsevier.com/locate/ceramint

Short communication

Ultra-flexible polymethyl methacrylate composites induced by sliding of micron-sized hexagonal boron nitride platelets

Bin-Huan Xie, Xiao Huang*, Guo-Jun Zhang*

State Key Laboratory of High Performance Ceramics and Superfine Microstructures, Shanghai Institute of Ceramics, Shanghai 200050, China

Received 8 March 2013; received in revised form 12 March 2013; accepted 21 March 2013
Available online 6 April 2013

Abstract

An ultra-flexible hexagonal boron nitride (h-BN)/ polymethyl methacrylate (PMMA) composite with extra-large elongation at rupture was prepared by introducing micron-sized surface-modified h-BN platelets into a PMMA matrix. At 32 wt% loading of surface-modified h-BN, the composite can be folded freely and has an elongation at rupture of 68%, which is over 30 times larger than that of PMMA. Such results are due to the lubricant nature and the sliding of h-BN platelets.

Keywords: B. Composites; B. Hexagonal boron nitride platelets; C. Mechanical properties

1. Introduction

Hexagonal boron nitride (h-BN) is a structural analog and the isoelectronic counterpart of graphite. Like graphite, it possesses many exceptional in-plane properties such as high bulk modulus, high thermal conductivity, etc., which can lead to numerous applications [1–3]. For example, h-BN is often introduced into a polymer matrix as inorganic fillers in an attempt to improve the properties of the composites. Various types of h-BN, including, but not limited to, micro-particles, nanotubes, nanosheets, etc., have been tried to make high-performance polymer composites, especially high-thermal-conductivity polymer composites [4–8].

Generally, when hard inorganic fillers are introduced into a polymeric matrix, thermal conductivity, thermal stability, hardness and many mechanical properties of the composites will increase, while the flexibility and elongation at rupture will decrease. The reduction of flexibility and elongation at rupture is due to the restriction of the motion of polymer chains by the fillers [9–11]. Nielsen proposed a model to predict the decrease of the elongation at rupture of the polymer matrix composites at different filler loadings [12]. Nielsen's equation is described as $\varepsilon_c/\varepsilon_m = 1-\varphi_f^{1/3}$, where ε_c and ε_m are the elongations at rupture of the composite and matrix respectively and φ_f is the volume fraction of the filler. Based upon Nielsen's model, the elongation of the composite is always smaller than that of the matrix, with very few exceptions [13].

Here, we report a hydrothermal method to perform a surface modification on h-BN platelets and a simple procedure to prepare the surface-modified h-BN/PMMA composites. Interestingly, the composite at 32 wt% h-BN loading shows ultra-flexibility and extraordinary large elongation at rupture. Detailed studies were carried out and a mechanism was proposed to explain this rare phenomenon.

2. Experimental

In order to enhance the interfacial interactions between h-BN and the polymer matrix, h-BN was first surface-modified, similarly to the modification of BNNTs by Zhi et al. [14]. h-BN (SICCAS, Shanghai, China; purity > 99.5%, ~0.6 μm) was mixed with 30% hydrogen peroxide (Guoyao Chemicals Co. Ltd., Shanghai, China; AR grade) at 0.1 g/ml. The mixture was sealed in an autoclave and stirred for 24 h. And then, the mixture was heated up to 100 °C and kept at that temperature for 24 h. After being cooled to room

*Corresponding authors. Tel.: +86 21 52411080/52414318; fax: +86 21 52413122.
E-mail addresses: xiaohuang@mail.sic.ac.cn (X. Huang), gjzhang@mail.sic.ac.cn (G.-J. Zhang).

0272-8842/$ - see front matter © 2013 Elsevier Ltd and Techna Group S.r.l. All rights reserved.
http://dx.doi.org/10.1016/j.ceramint.2013.03.076

temperature, the mixture was filtered and washed by deionized water three times, and then dried at 50 °C under vacuum. To prepare the composites, the desired amount of BN was added to 45 ml methyl methacrylate (Guoyao Chemicals Co. Ltd., Shanghai, China; CP grade, used as received) monomer, and sonicated for 5 min before 42 mg α-α'-azoic-isobutyronitrile (Guoyao Chemicals Co. Ltd., Shanghai, China; CP grade, used as received) was added. After being stirred at 90 °C for 90 min, the viscous mixture was poured into a Teflon mold and sealed. The mold was then placed in an oven at 50 °C for 48 h, and 100 °C for another 24 h. After cooling, the composites were obtained. Each sample was processed under the same conditions.

The SEM images were taken by a Hitachi S-570 scanning electron microscope. The mechanical properties were evaluated by a universal material testing machine (Instron-5566). The thicknesses of the samples containing 0, 8, 13, and 32 wt% m-BN were measured to be 0.225, 1.421, 0.525, and 0.251 mm, respectively, and uniform along the length of the strip. Tests were performed at a rate of 10 mm/min. Fourier transform infrared (FT-IR) spectra were taken with a Thermo Nicolet Nexus spectrometer between 400 and 4000 cm^{-1}. XRD patterns were recorded via a Rigaku X-ray diffractometer (D/Max-2250 V) using CuKα radiation. Photographs were taken by a SONY DSC-S800 digital camera.

3. Results and discussion

FT-IR spectra of pristine h-BN (p-BN) and surface-modified h-BN (m-BN) are shown in Fig. 1a. Two strong characteristic absorption bands of h-BN can be clearly identified. The peak around 1377 cm^{-1} is due to B–N stretching vibrations, while the peak at 814 cm^{-1} is attributed to the B–N–B out-of-plane bending [15]. After surface modification, a new absorption band at 2021 cm^{-1} can be observed in m-BN, which probably corresponds to some types of boron and oxygen bonding [16,17], coming from the reaction with hydrogen peroxide. Zeta potential measurements show that after surface modification, zeta potential changes from −39.45 mV to −51.50 mV, also indicating significant surface properties change. A larger zeta potential usually means better dispersibility [18].

According to the XRD profiles in Fig. 1b, the BN crystal structure does not change before and after surface modification. However, there are notable changes in h-BN morphologies seen by SEM. Before surface modification, the p-BN shows perfect platelet morphology. The edges of the platelets are smooth and intact (Fig. 1c). After surface modification, the edges of many m-BN platelets show clear layered structures (Fig. 1d). It seems that h-BN layers, which perfectly stacked with each other previously, slide to some extent with respect to each other during the hydrothermal surface modification process.

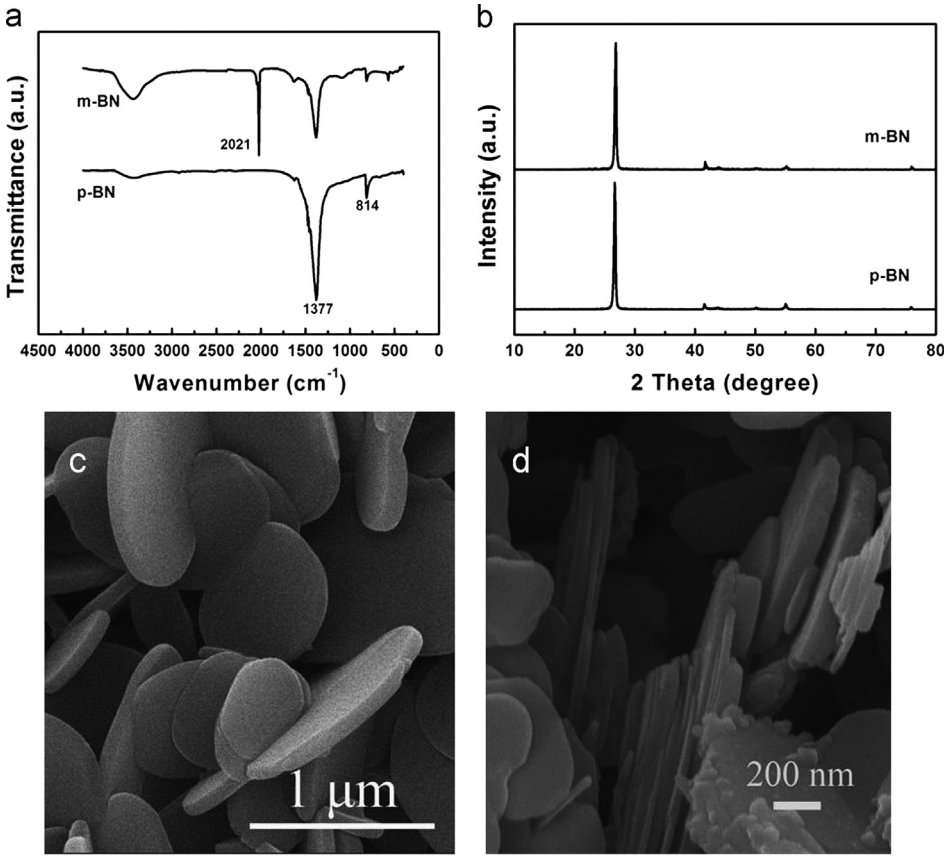

Fig. 1. (a) FT-IR spectra and (b) XRD profiles of pristine h-BN (p-BN) and surface-modified h-BN (m-BN); SEM images of (c) p-BN and (d) m-BN.

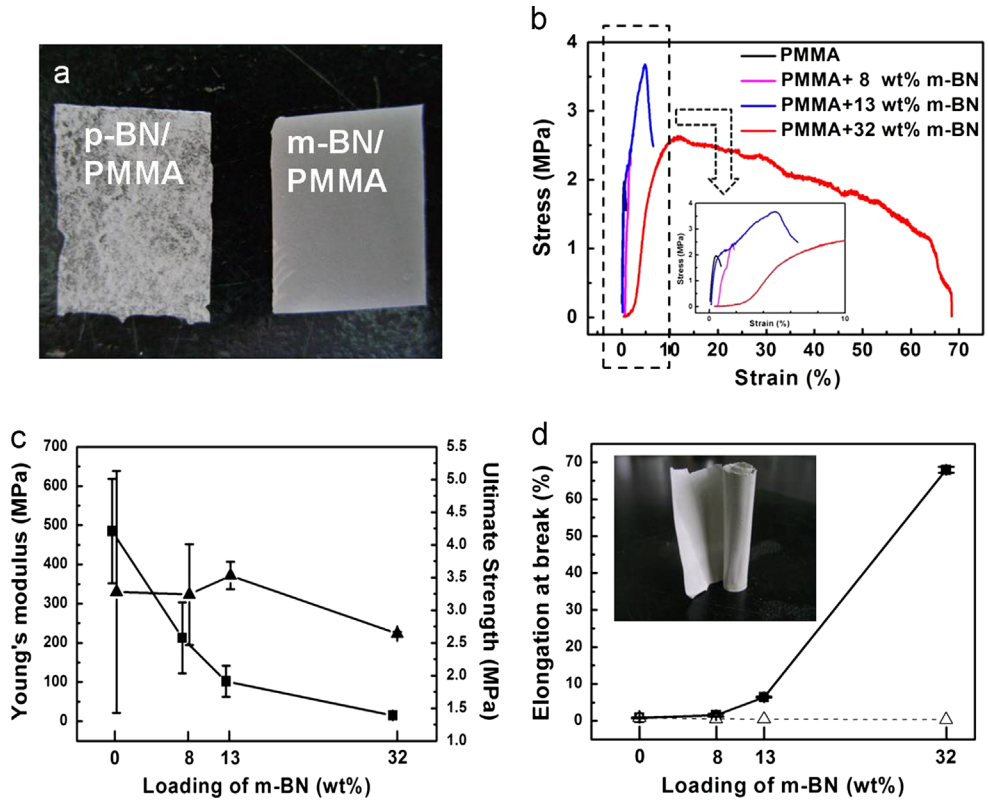

Fig. 2. (a) Photographs of composites with solids loading of 0.2 wt% BN; (b) stress–strain curves of PMMA and its composites, inset: expansions near 0% stress; (c) ultimate strengths (▲) and Young's moduli (■); (d) the experimental (■) and calculated (△) (based on the Nielsen equation) elongation at rupture of the composites versus m-BN loading, inset: photograph of the m-BN/PMMA composite film (0.25 mm thick) with 32 wt% m-BN loading.

Photographs of BN/PMMA composites are shown in Fig. 2a. Apparently, m-BN particles distribute more homogeneously in the PMMA matrix than p-BN. This is because, after surface modification, the new bondings on the surface of m-BN enhanced their interaction with the polymer matrix, and the larger zeta potential of m-BN leads to better dispersibility in the polymer matrix [14,18]. Meanwhile, there are no apparent agglomerations of the BN flakes, and they exist in the form of single flakes. And when increasing the p-BN loading to 24 wt%, the composite just broke into pieces after polymerization. Thus, we focus our research on m-BN/PMMA composites.

The stress–strain curves of three m-BN/PMMA composites and pristine PMMA are shown in Fig. 2b. Ultimate strengths and Young's moduli of the composites versus m-BN loadings are summarized in Fig. 2c.

It seems that the tensile strengths of the composites decrease after h-BN micro-platelets are introduced into the polymer matrix. Based on a simple shear lag model, the applied load during stretching is transferred to the inorganic platelets through shear stresses developed in the polymer matrix. The ultimate tensile strength of the composite δ_c can be described as $\delta_c = \alpha V_p \delta_p + (1-V_p)\delta_m$, where δ_p and δ_m are ultimate tensile strengths of the inorganic platelet and the polymer matrix, respectively, V_p is the volume fraction of platelet fillers and α is a parameter related to the aspect ratio of the platelet and is always less than one [19,20]. Since h-BN layers are held together by weak Van der Waals forces [21], it makes sense that the tensile strengths of the composites are lower than that of the polymer. Young's modulus also decreases as h-BN loading increases.

The experimental and calculated (based on the Nielsen equation) elongations at rupture of the composites versus BN loadings are presented in Fig. 2d. It is reported that when 30 vol% h-BN was introduced into HDPE, the elongation at rupture dropped from original 650% to only 45% [22]. Such drops are even much greater than predictions from Nielsen's equation [12]. But in our case, the elongation at rupture of the composites increases significantly with the m-BN loading, which is rather rare.

The increase in elongation at rupture of our system seems to be much more dramatic at higher m-BN loadings. At 32 wt% m-BN loading, the corresponding composite becomes so flexible that a 0.25-mm-thick composite film can be folded freely without breaking it, just like a piece of tape (see Fig. 2d inset). At higher loadings, m-BN may form a continuous phase, which might contribute to the super-flexibility. Unfortunately, the viscosity of the h-BN/MMA mixture increases very fast with the increase of h-BN loading. The processability of the high h-BN loading composites becomes very poor. Thus 32 wt% BN loading is the highest loading we studied.

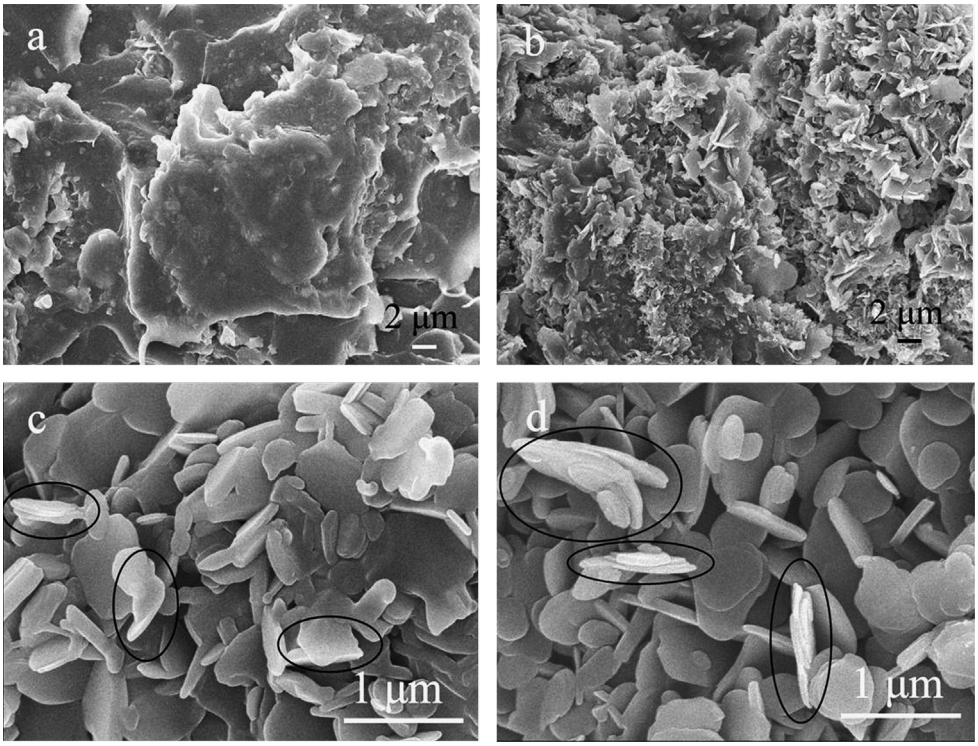

Fig. 3. SEM images of snapped cross sections of (a) p-BN/PMMA composite (7 wt% loading) and (b) m-BN/PMMA composite (32 wt% loading); (c) higher magnification SEM of (b); (d) BN powder from m-BN/PMMA composite (32 wt% BN loading) being stretched to break and then calcined at 600 °C (circles are curled edges and sliding layers).

Snapped cross sections of a brittle p-BN/PMMA composite and a flexible m-BN/PMMA composite (32 wt% m-BN loading) were carefully examined by SEM. SEM images in Fig. 3a and b reveal that the fracture behavior of two BN/PMMA composites is totally different. In Fig. 3a, the cross section of the brittle p-BN/PMMA composite is smooth, typical of brittle fracture [23], which is similar to that of PMMA. It reveals that when the sample is stretched, the fracture of a p-BN/PMMA composite is basically determined by the PMMA matrix. The elongation at rupture and tensile strength are also close to those of PMMA.

However, Fig. 3b tells a different story. The cross section of the m-BN/PMMA composite becomes much rougher. The flake-like particles in Fig. 3b are obviously m-BN microplatelets. Actually, the cross section of the flexible m-BN/PMMA composite looks similar to the well-known "pull-out" phenomenon fiber-reinforced composites and ceramic composites in which particulate fillers are introduced to improve the fracture toughness of the brittle ceramic matrix [24,25]. As for platelet-reinforced polymer composites, it has been proposed that there are two failure modes. One is the platelet fracture mode which results from strong interactions between the inorganic fillers and the organic matrix and usually associates with strong but brittle materials. The other is the platelet pull-out mode which is due to the weak interfacial bondings and associates with weak but ductile materials [26,27]. In our cases, it seems that the h-BN platelets are also being pulled out of the polymer matrix. But, there are actually more happenings in our system.

Fig. 3c gives a closer look at the BN particles at the fracture section in Fig. 3b. Compared with original m-BN particles (Fig. 1d), besides layered structures, several obvious changes can be noticed. The BN platelets at the fracture section seem to become thinner than original platelets and some curly edges are present. In order to remove the possible illusion from PMMA, one composite film with 32 wt% m-BN loading was stretched to break and then calcined at 600 °C. Thinner platelets and curly and layered structures are clearly present in the SEM images of the obtained powder (Fig. 3d), which is proved to be h-BN by XRD (Fig. 4a; top).

Based upon SEM observations, it seems that the h-BN layers in the composites can slide by the shear force during stretching. As shown in Fig. 4a, the *d*-spacing of the layer distance of BN in the m-BN/PMMA composite is slightly larger than that of p-BN/PMMA, p-BN and m-BN. It seems that due to stronger interactions, methyl methacrylate molecules can "swell" the m-BN and the "swelling" disappears upon removal of PMMA. Based upon Lifshitz's model, such an increase in *d*-spacing will lead to about 5% loss of binding energy between BN layers [28,29]. Apparently, the Van der Waals forces between the layers of m-BN in m-BN/PMMA composites are weakened and the layers become more slidable/peelable. Due to these changes, the Van der Waals forces between the BN layers may become weaker than the bonding forces between m-BN and the PMMA matrix and the strength of PMMA itself.

During stretching, as a proposed hypothesis illustrated in Fig. 4b, the stress applied on the composite is transferred to h-

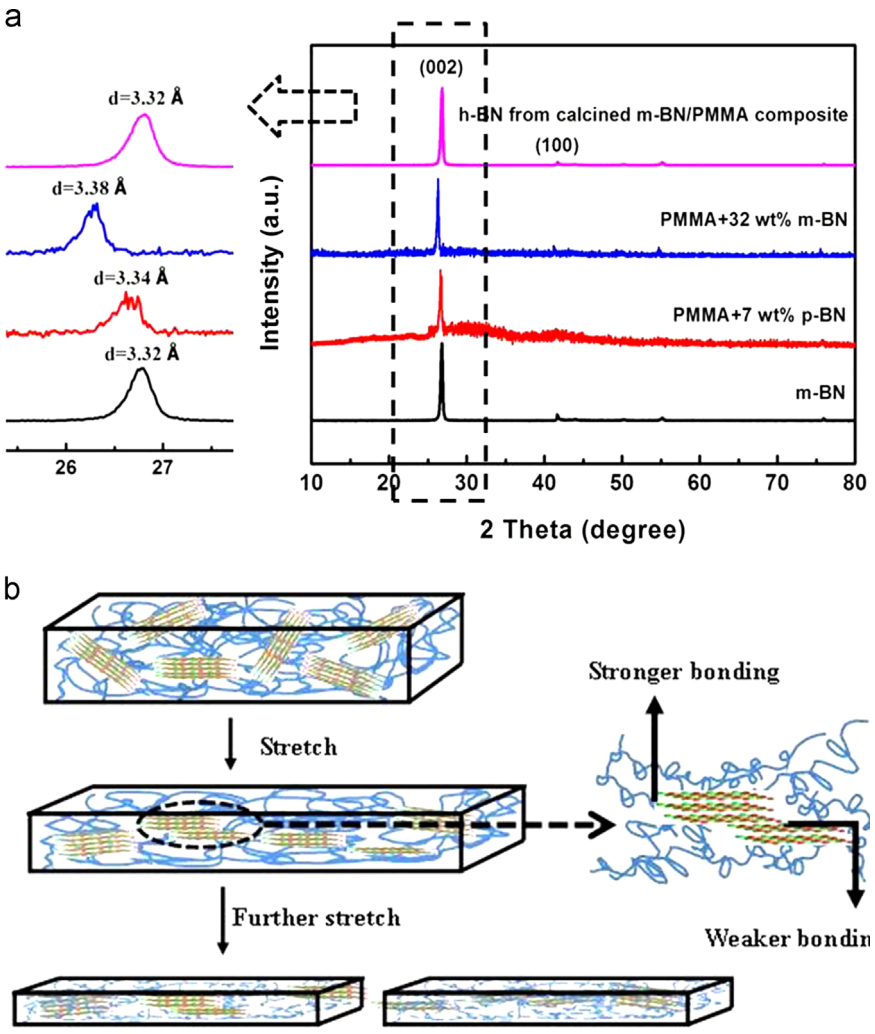

Fig. 4. (a) XRD patterns of m-BN, BN/PMMA composites and BN from m-BN/PMMA (32 wt% BN loading) composite film being stretched to break followed by calcination at 600 °C and (b) proposed mechanism of m-BN/PMMA composite during stretching.

BN platelets by shear stresses developed in the matrix [19]. The m-BN platelets as the weakest link yield first to slide to form visible (by SEM) layered structures. Ultimate slide leads to layers being peeled off from each other to form thinner BN platelets. The curly features come from the released stress after break. Sliding of m-BN layers seems to be the most possible reason for the uncommon increase of the elongation at rupture in the m-BN/PMMA composite. Our approach seems to provide a possible pathway to weaken the binding force between h-BN layers.

4. Conclusions

In summary, an ultra-flexible h-BN/PMMA composite was prepared by introducing surface-modified h-BN into a PMMA matrix. At 32 wt% BN loading the elongation at rupture of the m-BN/PMMA composite, which can be folded freely, is increased to 68%, over 30 times higher than that of original PMMA. The extraordinary increase of the elongation at rupture and super-flexibility of the composites are results from the delicate balance among the interaction strengths of h-BN layers, inorganic–organic interfaces which are strongly affected by the surface modification and the morphology of the fillers (shape and aspect ratio). During stretching, the composite fails as the platelets "pull out" with obvious sliding. It suggests a potential general route to improve the flexibility of polymer composites.

Acknowledgments

Financial support from the Chinese Academy of Science (Hundred Talents Program) and Science and Technology Commission of Shanghai Municipality (#11ZR1442200) is gratefully acknowledged.

References

[1] G.J. Zhang, J.F. Yang, M. Ando, T. Ohji, S. Kanzaki, Reactive synthesis of alumina–boron nitride composites, Acta Materialia 52 (2004) 1823–1835.

[2] J.X. Xue, J.X. Liu, B.H. Xie, G.J. Zhang, Pressure-induced preferential grain growth, texture development and anisotropic properties of hot pressed hexagonal boron nitride ceramics, Scripta Materialia 65 (2011) 966–969.

[3] Y.K. Shin, et al., Effect of BN filler on thermal properties of HDPE matrix composites, Ceramics International (2012).
[4] S.L.C. Hsu, T.L. Li, Journal of Physical Chemistry B 114 (2010) 6825–6829.
[5] T.C. Mo, H.W. Wang, S.Y. Chen, Y.C. Yeh, Synthesis and dielectric properties of polyaniline/titanium dioxide nanocomposites, Ceramics International 34 (2008) 1767–1771.
[6] C.Y. Zhi, Y. Bando, T. Terao, C.C. Tang, H. Kuwahara, D. Golberg, Advanced Functional Materials 19 (2009) 1857–1862.
[7] T. Nakayama, H.B. Cho, Y. Tokoi, S. Endo, S. Tanaka, T. Suzuki, W.H. Jiang, H. Suematsu, K. Niihara, Composites Science and Technology 70 (2010) 1681–1686.
[8] Y. Song, C. Yang, D.B. Liu, Y.H. Lin, C.W. Nan, Self-orientation of graphite-nanoplates induces anisotropy of nanoplates–epoxy composites, Ceramics International 38 (2012) S91–S94.
[9] K. Sato, H. Horibe, T. Shirai, Y. Hotta, H. Nakano, H. Nagai, K. Mitsuishi, K. Watari, Thermally conductive composite films of hexagonal boron nitride and polyimide with affinity-enhanced interfaces, Journal of Materials Chemistry 20 (2010) 2749–2752.
[10] F. Gayet, L. Viau, F. Leroux, F. Mabille, S. Monge, J.J. Robin, A. Vioux, Unique combination of mechanical strength, thermal stability, and high ion conduction in PMMA–silica nanocomposites containing high loadings of ionic liquid, Chemistry of Materials 21 (2009) 5575–5577.
[11] M.I. Sarwar, S. Zulfiqar, Z. Ahmad, Investigating the property profile of polyamide–alumina nanocomposite materials, Scripta Materialia 60 (2009) 988–991.
[12] L.E. Nielsen, R.F. Landel, Mechanical Properties of Polymers and Composites, Marcel Dekker Inc., New York, 1974.
[13] L.E. Nielsen, Dynamic mechanical-properties of polymers filled with agglomerated particles, Journal of Polymer Science Part B: Polymer Physics 17 (1979) 1897–1901.
[14] C.Y. Zhi, Y. Bando, T. Terao, C.C. Tang, H. Kuwahara, D. Golberg, Chemically activated boron nitride nanotubes, Chemistry—An Asian Journal 4 (2009) 1536–1540 Note: There is a huge exothermal process during the reaction. Slow heating is required. An inner cooling system is used to control the temperature when needed. Special attention should be paid due to safety issues.
[15] C.Y. Zhi, Y. Bando, C.C. Tang, D. Golberg, R.G. Xie, T. Sekiguchi, Large-scale fabrication of boron nitride nanohorn, Applied Physics Letters 87 (2005) 063107.
[16] C.Q. Miao, S.D.A. Li, $B_n(BO)_n^{2-}$, $CB_{n-1}(BO)_n^-$, and $C_2B_{n-2}(BO)_n$ ($n=5-12$): cage-like boron oxide clusters analogous to *closo*-$B_nH_n^{2-}$, $CB_{n-1}H_n^-$, and $C_2B_{n-2}H_n$, Science China Chemistry 54 (2011) 756–761.
[17] L. Andrews, T.R. Burkholder, Infrared-spectra of molecular $B(OH)_3$ and HOBO in solid argon, Journal of Chemical Physics 97 (1992) 7203–7210.
[18] H. Hu, A.P. Yu, E. Kim, B. Zhao, M.E. Itkis, E. Bekyarova, R. C. Haddon, Influence of the zeta potential on the dispersability and purification of single-walled carbon nanotubes, Journal of Physical Chemistry B 109 (2005) 11520–11524.
[19] L.J. Bonderer, A.R. Studart, L.J. Gauckler, Bioinspired design and assembly of platelet reinforced polymer films, Science 319 (2008) 1069–1073.
[20] H.L. Cox, The elasticity and strength of paper and other fibrous materials, British Journal of Applied Physics 3 (1952) 72–79.
[21] P. Lawrence, Some theoretical considerations of fiber pull-out from an elastic matrix, Journal of Materials Science 7 (1972) 1–6.
[22] W.Y. Zhou, S.H. Qi, H.D. Li, S.Y. Shao, Study on insulating thermal conductive BN/HDPE composites, Thermochimica Acta 452 (2007) 36–42.
[23] B. Wetzel, F. Haupert, M.Q. Zhang, Epoxy nanocomposites with high mechanical and tribological performance, Composites Science and Technology 63 (2003) 2055–2067.
[24] H. Jo, F.D. Blum, Characterization of the interface in polymer–silica composites containing an acrylic silane coupling agent, Chemistry of Materials 11 (1999) 2548–2553.
[25] J.J. Brennan, K.M. Prewo, Silicon–carbide fiber reinforced glass–ceramic matrix composites exhibiting high-strength and toughness, Journal of Materials Science 17 (1982) 2371–2383.
[26] D. Blond, V. Barron, M. Ruether, K.P. Ryan, V. Nicolosi, W.J. Blau, J.N. Coleman, Enhancement of modulus, strength, and toughness in poly (methyl methacrylate)-based composites by the incorporation of poly (methyl methacrylate)-functionalized nanotubes, Advanced Functional Materials 16 (2006) 1608–1614.
[27] L.S. Walker, V.R. Marotto, M.A. Rafiee, N. Koratkar, E.L. Corral, Toughening in graphene ceramic composites, ACS Nano 5 (2011) 3182–3190.
[28] H. Rydberg, M. Dion, N. Jacobson, E. Schroder, P. Hyldgaard, S.I. Simak, D.C. Langreth, B.I. Lundqvist, Van der Waals density functional for layered structures, Physical Review Letters 91 (2003) 126402.
[29] M.J. McAllister, J.L. Li, D.H. Adamson, H.C. Schniepp, A.A. Abdala, J. Liu, M. Herrera-Alonso, D.L. Milius, R. Car, R.K. Prud'homme, I.A. Aksay, Single sheet functionalized graphene by oxidation and thermal expansion of graphite, Chemistry of Materials 19 (2007) 4396–4404.